

Resolving the resolution of array CGH

Bradley P. Coe^{a,*}, Bauke Ylstra^b, Beatriz Carvalho^b, Gerrit A. Meijer^b,
Calum MacAulay^a, Wan L. Lam^a

^a British Columbia Cancer Research Centre, 675 West 10th Avenue, Vancouver, BC, Canada V5Z 1L3

^b VU University Medical Center, Amsterdam, The Netherlands

Received 7 November 2006; accepted 30 December 2006

Available online 2 February 2007

Abstract

Many recent technologies have been designed to supplant conventional metaphase CGH technology with the goal of refining the description of segmental copy number status throughout the genome. However, the emergence of new technologies has led to confusion as to how to describe adequately the capabilities of each array platform. The design of a CGH array can incorporate a uniform or a highly variable element distribution. This can lead to bias in the reporting of average or median resolutions, making it difficult to provide a fair comparison of platforms. In this report, we propose a new definition of resolution for array CGH technology, termed “functional resolution,” that incorporates the uniformity of element spacing on the array, as well as the sensitivity of each platform to single-copy alterations. Calculation of these metrics is automated through the development of a Java-based application, “ResCalc,” which is applicable to any array CGH platform.

© 2007 Elsevier Inc. All rights reserved.

Keywords: Nucleic acid hybridization; Genomic hybridizations; DNA arrays; Gene dosage; Loss of heterozygosity; Genetic techniques; Technology assessment

Array comparative genomic hybridization (aCGH) has rapidly supplanted conventional metaphase CGH as the standard protocol for identifying segmental copy number alterations in disease state genomes [1,2]. Currently, many genome-wide aCGH platforms are available that span the human genome at specific intervals to facilitate mapping of genetic alterations; however, these platforms are often described only by the number of elements present on the array or the average element spacing, which may not accurately reflect the relative performance of one platform to another, especially given the potential for highly variable element distribution throughout the genome being interrogated (Table 1) [2–12].

The primary concerns a user may have in selecting an aCGH platform for gene discovery are “What is the minimal alteration size that can be reliably detected?” “How precisely will the alteration boundaries be defined?” and “What are the sample requirements?” In this study we derive new performance definitions through the introduction of “functional resolution,” a new metric that incorporates the distribution of array data

points, and describe a Java-based application “ResCalc,” which automates the calculation of performance metrics for any aCGH platform (including any species and arrays covering only specific chromosomal segments). In addition, we discuss the practical performance characteristics and sample requirements of the major human aCGH platforms.

Results and discussion

Alteration detection is dependent on array element distribution

It is important to take into account the distribution and length of array elements to determine accurately the detection sensitivity to various alteration sizes (Fig. 1). A common practice is to utilize average or median element genomic spacing as a definition of resolution even when the distribution of array elements is nonuniform. However, it is an oversimplification to assume a uniform distribution of array elements and calculate resolution as the number of elements divided by the genome size [13]. Another misstatement is to define the resolution of an array by the length of the array elements. For example, it would be erroneous to claim that an

* Corresponding author. Fax: +1 604 675 8232.

E-mail address: bcoe@bccrc.ca (B.P. Coe).

Table 1
Comparison of array CGH technologies

Platform	Technology	Functional resolution			Sample labeling	Sample requirements	Notes
		Theoretical sensitivity	Single-copy sensitivity	Breakpoint precision			
Nimblegen 385K	Oligonucleotide (45–85 nt)	15 kb	54 kb*	24 kb	Whole genome	1–3 µg	*Single-copy sensitivity is estimated based on analysis parameters described in Selzer et al.
Agilent 244A	Oligonucleotide (60 nt)	36 kb	36 kb	56 kb	Whole genome	0.5 µg (1 µg with dye flip)	DNA amplification reduces DNA requirements to 0.1 µg of DNA per slide (0.2 µg with dye flip) (not tested in this study)
Affymetrix GeneChip human mapping 500K set	Oligonucleotide (25 nt)	41 kb	75 kb	74 kb	PCR reduction	0.5 µg	Platform is also used for LOH analysis
Submegabase Resolution Tiling (SMRT) set	Large insert clone (BAC)	50 kb	50 kb	152 kb	Whole genome	0.1 µg	High-level amplifications below 50 kb may be detectable; this is not indicated.
Affymetrix GeneChip human mapping 100K set	Oligonucleotide (25 nt)	271 kb	476 kb	528 kb	PCR reduction	0.5 µg	Platform is also used for LOH analysis
VUMC MACF human 30K	Oligonucleotide (60 nt)	1.05 Mb	1.32 Mb	1.94 Mb	Whole genome	0.3 µg	Invitrogen has recently released a 50K oligonucleotide library suitable for array CGH including intragenic oligonucleotides
Illumina Linkage IV	Oligonucleotide (40 nt)	1.35 Mb	2.66 Mb	2.06 Mb	PCR reduction	1 µg	Illumina has recently released a 100K (Infinium) assay. Both platforms are also used for LOH analysis.
UPenn	Large insert clone (BAC)	1.99 Mb	1.99 Mb	3.15 Mb	Whole genome	1 µg	Sample requirement is likely 100 ng due to use of BAC clones
Spectral Chip 2600	Large insert clones (BAC)	2.65 Mb	2.65 Mb	4.55 Mb	Whole genome	1 µg (2 µg with dye flip)	Sample requirement is likely 100 ng due to use of BAC clones
HumArray 3.2	Large insert clone (BAC)	5.07 Mb	5.07 Mb	8.75 Mb	Whole genome	0.6 µg	Sample requirement is likely 100 ng due to use of BAC clones

array consisting of 100-bp elements offers a resolution of 100 bp—unless every element was tiled contiguously. In this case the concept being relayed is the increased sensitivity of a single array element to a small alteration, not the overall resolution of the array. To cover the entire genome at this resolution would require approximately 30 million contiguous array elements. As this example demonstrates, a simple report of the number of measurements performed and the size of each

element is an unreliable method for determining the actual utility of a platform in detecting an alteration of a given size.

We propose that the detection sensitivity of an array is best described by the probability of detecting any alteration of a given size. As discussed by Davies et al. [2] the probability of detecting an alteration can be calculated for all possible alteration sizes by determining the percentage of alterations of a given size that would reside between adjacent array elements (Fig. 2A). Fig. 2B demonstrates the result of applying this definition to several key array platforms using the ResCalc algorithm. Tiling arrays using large-insert clones such as bacterial artificial chromosomes (BAC) demonstrate very robust performance due to the uniform distribution of elements across the genome and the presence of very few gaps in the genomic coverage [5,14] (Fig. 2B). Due to the reduced sensitivity of large-insert clones to alterations smaller than 50 kb, oligonucleotide platforms offer better theoretical performance in detecting small alterations [3,8,15]. The Nimblegen 385,000 oligonucleotide array offers the highest theoretical performance of all platforms, detecting 95% of 15-kb alterations (Fig. 2B). The probabilities of detecting alterations drop drastically for the lower density platforms at small alteration sizes, with the Affymetrix 100K platform detecting less than 55% of 27-kb alterations and 25% of 10-kb alterations (Fig. 2B).

Evaluation of practical performance

Due to various sources of experimental noise, optimal performance is rarely attainable for any array CGH platform.

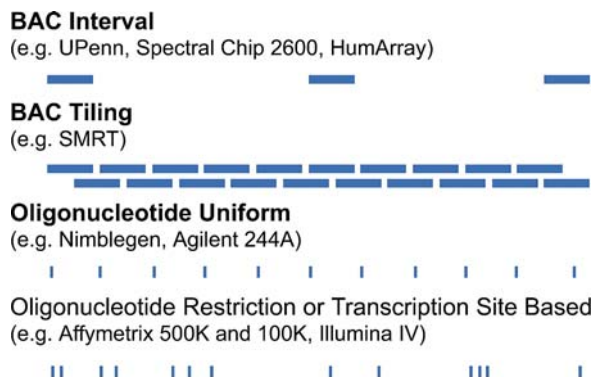


Fig. 1. Schematic overview of array CGH platform designs. BAC arrays are typically produced with uniform genomic distribution or with overlapping/tiling clones. Oligonucleotide arrays may also be produced with uniform genomic distribution; however, for some platforms the need for genome reduction labeling steps or design biased toward transcriptional sites leads to nonuniform element distribution causing local resolution to vary drastically.

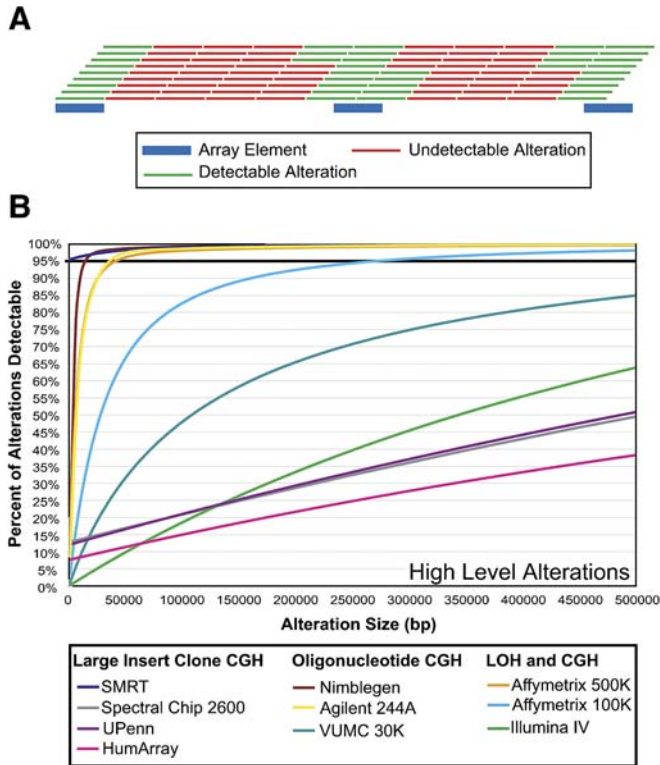


Fig. 2. Theoretical detection sensitivity. (A) Detection sensitivity for each array platform was calculated based on the percentage of possible alterations of a given size that interact with at least one array element (blue bars). To determine the proportion of alterations of size n bp detectable by an array platform we first defined the set of all possible alterations (possible alterations are represented by red and green bars) of size n bp for all genomic regions covered by the array (excluding centromeres and acrocentric regions). We then calculated the percentage of alterations not detectable as those that are completely contained within each coverage gap. (B) Detection sensitivities for each platform are plotted for alteration sizes from 1 to 500 kb; the alteration size at which a platform exceeds a 95% detection rate defines the optimal sensitivity of that platform.

Although high-level amplification may be readily detectable with all platforms regardless of noise, the ability to detect single-copy gains will be dependent on both the noise of the platform and the ratio response of each element. To detect a single-copy alteration with confidence, the average ratio for a region of copy number gain must differ from the average ratio for a normal portion of the genome by at least 1 standard deviation. When the intrinsic noise of a platform does not allow separation of single-copy alterations this can be compensated for through pooling multiple array elements by averaging to reduce the overall noise of the profile [16].

For cross-platform comparison of noise and ratio response, we use the human breast cancer cell line BT474, which has previously been characterized by high-resolution FISH mapping. It contains a near-tetraploid genome with 104 chromosomes per nucleus (an average of 4.5 copies of each chromosome) [17]. The ratio separation produced by a single-copy gain can be inferred by comparing chromosome bands 8p11–p12 and 8q22, which are present at 4 and 6 copies, respectively, in each BT474 nucleus (2:3 copy number ratio)

(Fig. 3A). Fig. 3B shows the copy number profiles for BT474 generated by expert groups using their preferred platforms. By calculating the average \log_2 ratio and standard deviation for 8p11–p12 and 8q22 and pooling various numbers of array elements, we can determine the performance of each platform. Fig. 3C demonstrates the results of comparing average \log_2 signal ratios based on individual and pooled elements for each platform. The SMRT array did not require pooling of elements and thus a single-copy change may be reliably detected by a single array element. This criterion is also applicable to the UPenn, Spectral Chip 2600, and HumArray v3.2 platforms, which use BACs as array elements. The Agilent 244A platform demonstrated the highest sensitivity of the oligonucleotide platforms, with a single element being sufficient to detect a single-copy alteration, while the Affymetrix and VUMC platforms required pooling of three and two elements, respectively, to allow separation of single-copy differences (Fig. 3C). It is worth noting that the Agilent 244A data represent the result of a dye flip array pair. To determine the effect of this transformation on functional resolution we compared the noise levels in the individual hybridizations to the averaged ratios (data not shown). Both of the hybridizations had noise levels sufficient to detect a single-copy change with a single array element (data for 8p11–p12 demonstrated between 0.9 and 1.1 times the standard deviation of the same region in the pooled data set). However, despite the minimal improvement to overall experimental noise in this example, it is worth noting that the single spot per locus design of the Agilent platform makes it difficult to determine if a single clone is a true positive or the result of a hybridization artifact without a replicate hybridization.

Data were not available for Nimblegen 385,000 element platform; as a result we utilized the definition provided by Selzer et al. to determine that at least five elements must be affected to detect a single-copy alteration [15].

Similarly, the Illumina Linkage IV platform performance is expected to be comparable to the Affymetrix platforms due to the use of short oligonucleotides and similar sample labeling technology [9].

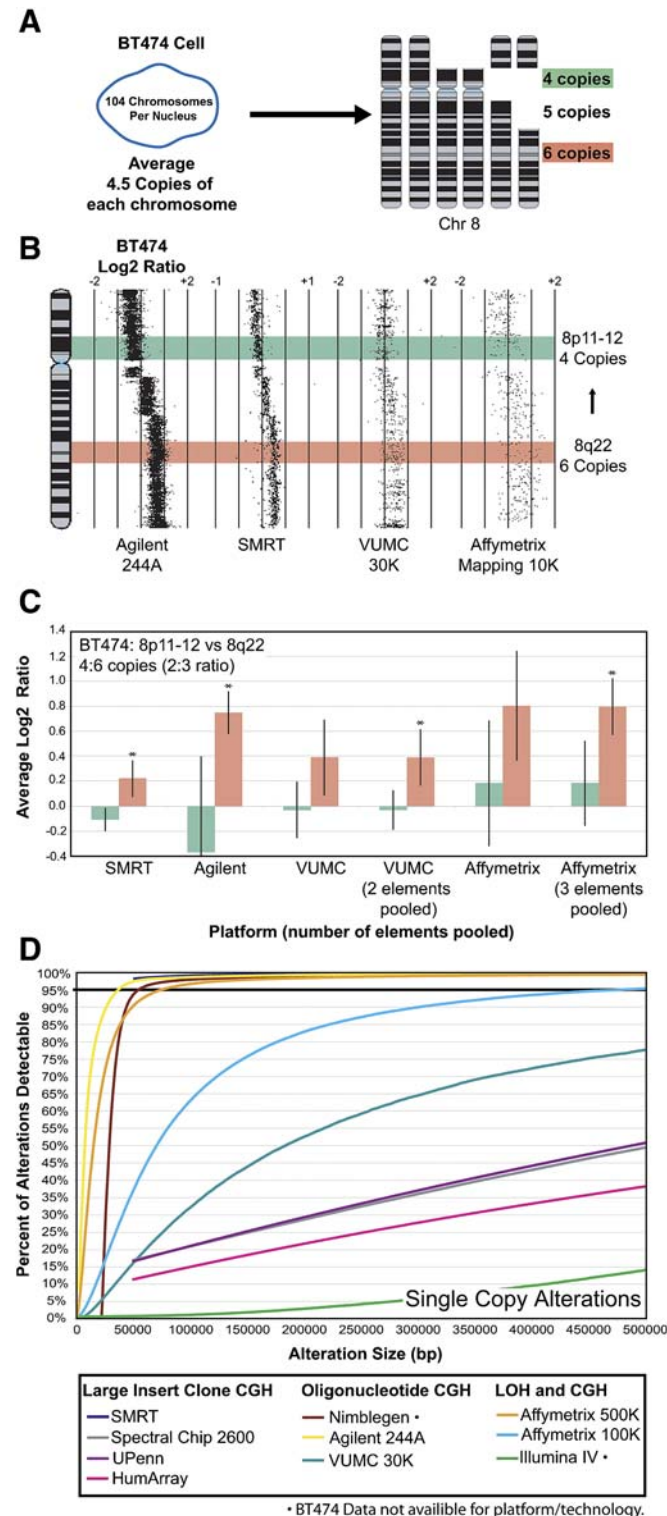
Fig. 3D demonstrates the output of ResCalc for several human array platforms, repeating the computation described for theoretical detection sensitivity and incorporating the need to pool various numbers of array elements to allow detection of single-copy alterations. Although high-level changes such as homozygous deletions and amplifications below 50 kb may be detectable with large insert clone arrays such as the SMRT, UPenn, Spectral Chip 2600, and HumArray v3.2 platforms, sensitivity to single-copy alterations is greatly reduced in this size range and this sensitivity is reflected by not calculating performance metrics below 50 kb.

Using this metric the Agilent 244A platform demonstrates the highest performance for single-copy alterations between 1 and 49 kb (8.7 to 97.5%). The SMRT array demonstrates the highest performance above 50 kb (98.2 to 99.9%). As alteration sizes approach 500 kb the Agilent 244A, SMRT, Nimblegen 385K, and Affymetrix 500K platforms demonstrate very similar performance (Fig. 3D).

Mapping of breakpoints is dependent on local resolution

In addition to concerns regarding the minimum alteration size that can be reliably detected, the user requires information regarding the precision with which the boundaries of an alteration can be defined. An optimal measurement of edge precision takes into account the fact that the mapping of an alteration boundary is dependent on the distance to the nearest

unaffected array element (Fig. 4A). In the case of overlapping array elements (for example, overlapping large-insert clones), breakpoints can be mapped to within a single array element and thus the intra- and interelement spacing should also be taken into account. Although the probability of detecting a breakpoint within an array element in an oligonucleotide platform or interval-based large-insert clone array element is lower, the reduced ratio response of a partially gained/lost clone may also be utilized in positioning a breakpoint. Thus, by incorporating the end-to-end spacing between each array element end, we can determine the proportion of the genome represented by intra/interelement intervals smaller than a given size. We can then determine the proportion of breakpoints (one potential breakpoint per nucleotide position in the genome) that can be defined with at least the threshold level of precision. This becomes our measurement of edge precision (Fig. 4A). Fig. 4B demonstrates the precision output of ResCalc for several key human aCGH platforms. We observe that increasing the number of array elements drastically changes the slope of the edge precision curve, resulting in a large proportion of edges being detectable at higher levels of precision. The current maximal theoretical performance is demonstrated by the use of the 385,000 oligonucleotide Nimblegen array, followed by the Agilent 244A and Affymetrix 500K arrays, with the relatively uniformly distributed clone ends on the SMRT array demonstrating the fourth best precision.



Defining functional resolution

It is apparent that increasing the number of array elements does not result in a linear increase in performance (Figs. 2–4). Factors including element size and uniformity of element distribution are key contributors to the theoretical performance of an array platform. In defining the functional resolution of an array platform, we propose integrating these metrics into the description of each technology. If we are analyzing samples in the context of mapping genetic alterations, it is prudent to

Fig. 3. Single-copy detection sensitivity. (A) The BT474 cell line contains an average of 4.5 copies of each chromosome. Previous FISH studies characterized chromosome 8 into segments with 4, 5, and 6 copies. Comparing the ratios observed for 6 and 4 copies we can simulate the performance of a 3:2 copy number ratio. (B) Comparison of copy number profiles of chromosome 8 across three platforms. (C) Determination of the number of elements that must be pooled to allow detection of single-copy alterations. BT474 profiles were used to determine the number of elements that must be pooled to separate the average ratios for 4 and 6 copies by at least 1 standard deviation (indicated by *) for the SMRT, Agilent, VUMC, and Affymetrix platforms (the noise of the Affymetrix Mapping 10K is projected to be equivalent to the 100K and 500K sets due to the use of genomic reduction steps and identical oligonucleotide design strategy). (D) Single-copy alteration detection sensitivities for each platform are plotted for alteration sizes from 1 to 500 kb; the alteration size at which a platform exceeds the 95% detection rate defines the optimal sensitivity of that platform. Each platform was penalized based on the number of elements that must be pooled according to the calculation described in (C). Data were not available for the Nimblegen platform; the data are adjusted to incorporate pooling of five elements as described in Selzer et al. [15]. Similarly, data were not available for the Illumina platform; due to the similar probe length and labeling technology compared to the Affymetrix platform, a three-clone requirement was assumed.

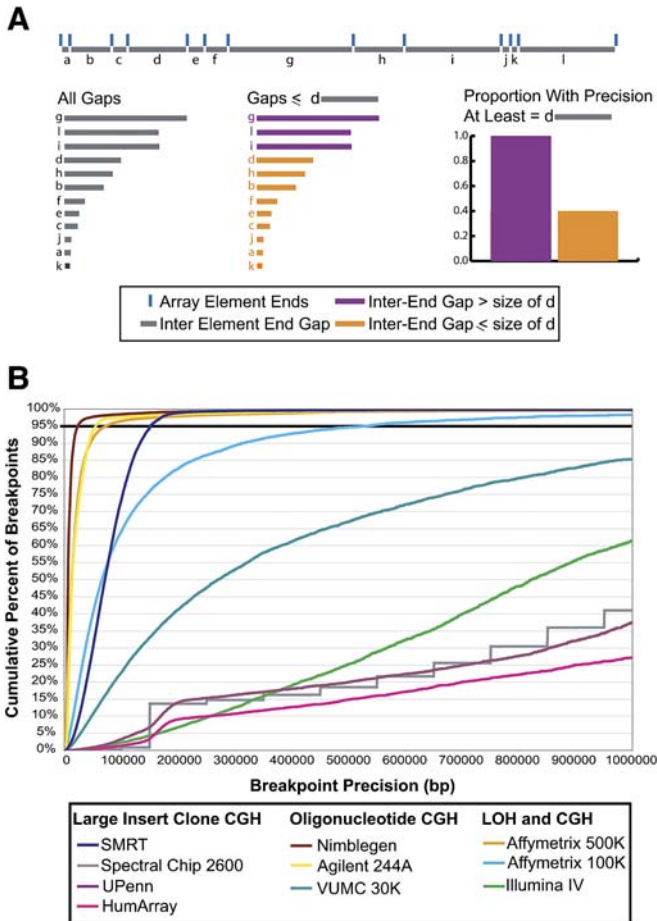


Fig. 4. Breakpoint precision. (A) The precision with which a breakpoint can be defined is derived from the genomic distance between each element end (as alteration boundaries can be defined to reside within an array element). The set of all interelement end gaps in the genome can then be determined (a to l) and sorted by increasing size. The percentage of the genome covered by interelement end gaps less than n bp in width (example size of gap “d”) defines the proportion of breakpoints that demonstrate a precision of at least n bp (assuming 1 possible breakpoint per base pair). (B) Breakpoint precisions for each platform are plotted for alteration sizes ranging from 1 kb to 1 Mb; the precision level at which a platform exceeds 95% defines the optimal breakpoint precision of that platform.

assume that resolution may be best defined by the level of performance (sensitivity and precision) that is applicable to describing 95% of genomic alterations. Thus the alteration size at which only 1 in 20 single-copy genomic alterations escape detection will define the practical sensitivity of a platform, while the alteration size at which 1 in 20 high-level copy number alterations escape detection defines the theoretical sensitivity. Incorporating these measurements as well as the precision demonstrated for 19 in 20 breakpoints will define the functional resolution of the platform (Figs. 2–4). Table 1 lists the functional resolutions (as determined by the ResCalc application) of all platforms discussed in this study. It is noteworthy that no one platform demonstrates the highest performance for all metrics at this time. The Nimblegen 385,000 element platform demonstrates the current maximum precision of 24 kb and theoretical resolution of 15 kb; however, single-copy alteration sensitivity is limited to 54-kb alterations.

Similarly the Agilent platform demonstrates the highest single-copy number alteration sensitivity of 36 kb; however, precision is limited to 56 kb (Table 1). It is obvious that oligonucleotide platforms demonstrate improved sensitivity to single-copy alterations as they increase their density; however, this is currently practical only for specific loci as whole human genome arrays with very high densities currently span more than two chips [15].

Sample considerations

A key consideration in selection of an aCGH platform is whether it is suitable for analyzing the type of samples at hand. Formalin-fixed paraffin-embedded (FFPE) samples are currently restricted to platforms that do not require probe complexity reduction steps (such as the Illumina and Affymetrix platforms). Currently low-yield FFPE samples are most applicable to large-insert clone platforms such as the SMRT array, while oligonucleotide platforms that lack genome-complexity reduction steps in probe generation may be capable of analyzing these samples as well, depending on attainable DNA yield [14,16]. Sample DNA amplification can drastically reduce the amount of primary material required; however, noise and bias are introduced by nonlinear amplification of sequences, limiting utility in the analysis of limited yield clinical specimens. Currently several platforms are capable of analyzing unamplified samples with limited yield (less than 1 μg), including all large-insert clone platforms (the Spectral Chip 2600 uses 1 μg of DNA if the dye flip experiment is excluded) and the VUMC and Affymetrix oligonucleotide platforms (including the Agilent 244A platform if the dye flip experiment is excluded).

Selecting a platform

It is important to note that attaining the highest possible resolution is not the only factor in determining the platform best suited to a particular analysis. High-resolution arrays demonstrate a significant cost increase over low-resolution platforms, which may be more appropriate depending on the hypothesis of the study at hand [16]. Another important consideration is the utility offered by combined LOH/CGH platforms, which can increase our understanding of cryptic copy number alterations (an important consideration is the percentage of heterozygous calls obtained in an average reference sample, which will determine the probability of generating a usable LOH call in a specific alteration) [8,9,18]. Taking these concerns into account as well as the theoretical and practical sensitivity, breakpoint precision, and sample requirements (both quality and DNA yield) will help determine the platform best suited to approach each biological hypothesis.

Conclusions

In this cautionary note, we highlight that the extrapolation of local resolution could misrepresent “functional resolution” of an aCGH platform across the genome. Our proposed metrics incorporate the distribution of array elements, allowing a more

objective comparison of array platforms. We envision that standard calculations of performance such as functional resolution as defined by ResCalc will prove invaluable in the future description/comparison of aCGH platforms.

Materials and methods

Array platform data sources

Array mapping files were obtained from the Gene Expression Omnibus (<http://www.ncbi.nlm.nih.gov/projects/geo/>) for the Agilent (GEO Accession No. GPL4091), VUMC (GEO Accession No. GPL2827), and Spectral Chip 2600 (GEO Accession No. GPL3780) platforms. Mappings were acquired from manufacturer Web sites for the Affymetrix 100K/500K (www.affymetrix.com), Illumina IV (www.illumina.com), HumArray 3.2 (cancer.ucsf.edu/array/services.php#humanBAC), SMRT (www.bccrc.ca/cg/ArrayCGH_Group.html), and UPenn (www.genomics.upenn.edu/people/faculty/weberb/CGH/html/downloads.htm) platforms. The Nimblegen 385K mapping was acquired from an internal hybridization results file.

For oligonucleotide platforms often only one mapping position is provided for an oligo; in this case the position of the second end is derived by adding 1 oligo size to the provided base pair position. In the case of the Nimblegen platform, which uses isothermic oligos of varying sizes, we based our calculations on an average 60-bp oligo length applied to each element. Similarly for the HumArray data, several BAC clones had only one base-pair position associated and the second end was assumed to be 150 kb distal.

BT474 data files were acquired from the following sources: SMRT (GEO Accession No. GSM69198), VUMC (GEO Accession No. GSM73557), Affymetrix (<http://research.dfc.harvard.edu/meyersonlab/snp/snp.htm>). The Agilent 244A data were generated from an averaged dye flip experiment performed by Agilent Technologies using their standard protocols (www.opengenomics.com) and have been submitted to GEO (GEO Accession No. GSE6415). Array data are also available from the System for Integrative Genomic Microarray Analysis (SIGMA) interactive Web database (<http://sigma.bccrc.ca>), which was used to generate the image in Fig. 3B [19].

Implementation of ResCalc

ResCalc is implemented as a command line-executable Java application. The application requires JRE 5.0 update 7.0 or better. Briefly, the application requires a tab-delimited text file describing the chromosomal position of each element present on the array and the base-pair coordinates of the start and end of each array element. Additionally a file that annotates the location of the centromere on each chromosome described in the platform file is required. There is no restriction on the number or names of chromosomes in either the platform or the centromere description file, thus the algorithm can be run on arrays covering any portion of the any genome. The executable, centromere description files for several human genome sequence builds and documentation are available at <http://sigma.bccrc.ca/ResCalc.html>.

Calculation of optimal detection sensitivity

The optimal detection sensitivity for a platform is calculated as follows.

First, the set of all interelement gaps is defined as the set of all positive differences between the end base-pair position of one array element and the start base-pair position of the next array element, excluding differences that include the centromere of the chromosome being examined. The number of potential alterations of a given size is defined such that one alteration may start at each unique base-pair position of the genome being interrogated.

The number of alterations of a given size that will be contained completely within a gap represents the alterations that will escape detection with the current array platform. This is calculated by subtracting the current alteration size from each interelement gap and summing the positive residuals.

The total size of the interrogated genome is then calculated as the sum of all center-to-center element intervals and is used to define the percentage of possible alterations that will be detected under optimal conditions as $1 - (\text{number of alterations missed}/\text{genome size})$.

Calculation of practical detection sensitivity

The first step in calculating the practical sensitivity for an array platform is to determine the number of elements that must be averaged to reduce the variation in the data enough to allow detection of a single-copy alteration (defined as separating a region of normal copy number from a region of single-copy gain by 1 standard deviation).

The calculation is then performed similar to the calculation for optimal detection sensitivity with the following modifications. The number of clones that must be averaged to detect a single-copy change defines the penalty. The interelement gaps are defined as the set of positive differences between the end base-pair position of one element and the start base-pair position of the element exactly $n - 1$ elements away. If this spacing is greater than the alteration size being interrogated the number of alterations missed is defined as follows:

If the base-pair start position of the next element outside of the penalty window – the alteration size is less than the base-pair position of the end of the next clone, the number of alterations missed is defined as the interval between the end of the current clone and the position defined above. Otherwise the number of alterations missed is defined as the interval between the current element's end base-pair position and the end base-pair position of the next array element.

Calculation of breakpoint precision

The percentage of breakpoints that may be mapped with a precision of at least n bp is defined as the cumulative distribution of interelement end base-pair intervals (excluding intervals that span a centromere) $>$ the currently interrogated level of precision.

Acknowledgments

The authors thank Timon Buys, Raj Chari, Jonathan Davies, Ron deLeeuw, Will Lockwood, and Ian Wilson (BCCRC), for careful proofreading of the manuscript, and Eric Lin of Agilent Technologies for providing the unpublished BT474 hybridization. This work was supported by funds from Genome Canada/British Columbia, the Canadian Institutes of Health Research, and NIDCR (R01 DE015965). B.P.C. is supported by scholarships from the Natural Sciences and Engineering Research Council and the Michael Smith Foundation for Health Research.

References

- [1] D.G. Albertson, D. Pinkel, Genomic microarrays in human genetic disease and cancer, *Hum. Mol. Genet.* 12 (2) (2003) R145–R152.
- [2] J.J. Davies, I.M. Wilson, W.L. Lam, Array CGH technologies and their applications to cancer genomes, *Chromosome Res.* 13 (2005) 237–248.
- [3] M.T. Barrett, A. Scheffer, A. Ben-Dor, N. Sampas, D. Lipson, R. Kincaid, P. Tsang, B. Curry, K. Baird, P.S. Meltzer, Z. Yakhini, L. Bruhn, S. Laderman, Comparative genomic hybridization using oligonucleotide microarrays and total genomic DNA, *Proc. Natl. Acad. Sci. USA* 101 (2004) 17765–17770.
- [4] J. Greshock, T.L. Naylor, A. Margolin, S. Diskin, S.H. Cleaver, P.A. Futreal, P.J. deJong, S. Zhao, M. Liebman, B.L. Weber, 1-Mb resolution array-based comparative genomic hybridization using a BAC clone set optimized for cancer gene analysis, *Genome Res.* 14 (2004) 179–187.
- [5] A.S. Ishkanian, C.A. Malloff, S.K. Watson, R.J. DeLeeuw, B. Chi, B.P. Coe, A. Snijders, D.G. Albertson, D. Pinkel, M.A. Marra, V. Ling, C. MacAulay, W.L. Lam, A tiling resolution DNA microarray with complete coverage of the human genome, *Nat. Genet.* 36 (2004) 299–303.
- [6] A.M. Snijders, N. Nowak, R. Segraves, S. Blackwood, N. Brown, J. Conroy, G. Hamilton, A.K. Hindle, B. Huey, K. Kimura, S. Law, K.

- Myambo, J. Palmer, B. Ylstra, J.P. Yue, J.W. Gray, A.N. Jain, D. Pinkel, D.G. Albertson, Assembly of microarrays for genome-wide measurement of DNA copy number, *Nat. Genet.* 29 (2001) 263–264.
- [7] A.M. Snijders, B.L. Schmidt, J. Fridlyand, N. Dekker, D. Pinkel, R.C. Jordan, D.G. Albertson, Rare amplicons implicate frequent deregulation of cell fate specification pathways in oral squamous cell carcinoma, *Oncogene* 24 (2005) 4232–4242.
- [8] X. Zhao, B.A. Weir, T. LaFramboise, M. Lin, R. Beroukhim, L. Garraway, J. Beheshti, J.C. Lee, K. Naoki, W.G. Richards, D. Sugarbaker, F. Chen, M.A. Rubin, P.A. Janne, L. Girard, J. Minna, D. Christiani, C. Li, W.R. Sellers, M. Meyerson, Homozygous deletions and chromosome amplifications in human lung carcinomas revealed by single nucleotide polymorphism array analysis, *Cancer Res.* 65 (2005) 5561–5570.
- [9] E.H. Lips, J.W. Dierssen, R. van Eijk, J. Oosting, P.H. Eilers, R.A. Tollenaar, E.J. de Graaf, R. van't Slot, C. Wijmenga, H. Morreau, T. van Wezel, Reliable high-throughput genotyping and loss-of-heterozygosity detection in formalin-fixed, paraffin-embedded tumors using single nucleotide polymorphism arrays, *Cancer Res.* 65 (2005) 10188–10191.
- [10] P. van den Ijssel, M. Tijssen, S.F. Chin, P. Eijk, B. Carvalho, E. Hopmans, H. Holstege, D.K. Bangarusamy, J. Jonkers, G.A. Meijer, C. Caldas, B. Ylstra, Human and mouse oligonucleotide-based array CGH, *Nucleic Acids Res.* 33 (2005) e192, 1–9.
- [11] M.M. Weiss, E.J. Kuipers, C. Postma, A.M. Snijders, D. Pinkel, S.G. Meuwissen, D. Albertson, G.A. Meijer, Genomic alterations in primary gastric adenocarcinomas correlate with clinicopathological characteristics and survival, *Cell Oncol.* 26 (2004) 307–317.
- [12] I. Braude, B. Vukovic, M. Prasad, P. Marrano, S. Turley, D. Barber, M. Zielenska, J.A. Squire, Large scale copy number variation (CNV) at 14q12 is associated with the presence of genomic abnormalities in neoplasia, *BMC Genomics* 7 (2006) 138, 1–9.
- [13] Y. Nannya, M. Sanada, K. Nakazaki, N. Hosoya, L. Wang, A. Hangaishi, M. Kurokawa, S. Chiba, D.K. Bailey, G.C. Kennedy, S. Ogawa, A robust algorithm for copy number detection using high-density oligonucleotide single nucleotide polymorphism genotyping arrays, *Cancer Res.* 65 (2005) 6071–6079.
- [14] C. Garnis, B.P. Coe, S.L. Lam, C. MacAulay, W.L. Lam, High-resolution array CGH increases heterogeneity tolerance in the analysis of clinical samples, *Genomics* 85 (2005) 790–793.
- [15] R.R. Selzer, T.A. Richmond, N.J. Pofahl, R.D. Green, P.S. Eis, P. Nair, A.R. Brothman, R.L. Stallings, Analysis of chromosome breakpoints in neuroblastoma at sub-kilobase resolution using fine-tiling oligonucleotide array CGH, *Genes Chromosomes Cancer* 44 (2005) 305–319.
- [16] B. Ylstra, P. van de IJssel, B. Carvalho, G.A. Meijer, BAC to the future! or Oligonucleotides: a perspective for micro array comparative genomic hybridization (array CGH), *Nucleic Acids Res.* 32 (2006) 445–450.
- [17] D.J. Venter, S.J. Ramus, F.M. Hammet, M. de Silva, A.M. Hutchins, V. Petrovic, G. Price, J.E. Armes, Complex CGH alterations on chromosome arm 8p at candidate tumor suppressor gene loci in breast cancer cell lines, *Cancer Genet. Cytogenet.* 160 (2005) 134–140.
- [18] X. Zhao, C. Li, J.G. Paez, K. Chin, P.A. Janne, T.H. Chen, L. Girard, J. Minna, D. Christiani, C. Leo, J.W. Gray, W.R. Sellers, M. Meyerson, An integrated view of copy number and allelic alterations in the cancer genome using single nucleotide polymorphism arrays, *Cancer Res.* 64 (2004) 3060–3071.
- [19] R. Chari, W.W. Lockwood, B.P. Coe, A. Chu, D. Macey, A. Thomson, J.J. Davies, C. Macaulay, W.L. Lam, SIGMA: a system for integrative genomic microarray analysis of cancer genomes, *BMC Genomics* 7 (324) (2006) 1–11.